Supporting Information

Boron Enhances Oxygen Evolution Reaction Activity over Ni Foam-Supported Iron Boride Nanowires

Qinghua Liu,[a,b] Hui Zhao,[a] Meng Jiang,[a] Qing Kang,[*a] Wei Zhou,[*c] Pengcheng Wang,[a] Feimeng Zhou[a]

[a]*Institute of Surface Analysis and Chemical Biology, University of Jinan, Jinan, Shandong 250022, P. R. China*

[b]*College of Chemistry and Chemical Engineering, Central South University, Changsha, Hunan 410083, P. R. China*

[c]*Department of Applied Physics, Tianjin Key Laboratory of Low Dimensional Materials Physics and Preparing Technology, Tianjin University, Tianjin, 300072, P.R. China*

[*] Corresponding author E-mail: ila_kangq@ujn.edu.cn

[*] Corresponding author E-mail: weizhou@tju.edu.cn

Experimental Details

Chemicals and Materials

Ni Foams (NFs, 99.9% purity, 98% porosity, and 1.80 mm in thickness) and Ni plates (99.9% purity and 1.80 mm in thickness) were purchased from Incoatm Co. Ltd (Shenyang, China). A Pt plate (purity ≥ 99.99% and 0.2 mm in thickness) and a graphite plate (99.95% purity and 0.2 mm in thickness) were acquired from Ida Co. Ltd (Tianjin, China). HCl, KOH, NaOH, $FeCl_2 \cdot 4H_2O$, $NaBH_4$, and other reagents were of analytical grade and purchased from Aladdin Co. Ltd (Shanghai, China) and used as received. Deionized water was used throughout the experiments.

Electrocatalyst preparation

NFs were ultrasonically cleaned with 3 M HCl solution, 95% ethanol, and deionized water three times to remove nickel oxide and other impurities. Each piece of NF (20 × 10 × 1.8 mm) was immersed in a metal precursor aqueous solution containing 0.70 M $FeCl_2 \cdot 4H_2O$. Each NF was placed inside a reaction vessel with the surface normal to the magnetic field from a magnetic stirrer (magnetic intensity of 15 mT). The reaction vessel was maintained below 10 ^oC in an ice-bath. A mixture of 0.70 M $NaBH_4$ and 0.25 M NaOH was slowly added into the metal precursor aqueous solution using a syringe until a 1:1 volumetric ratio was reached. Fe_2B NWs were deposited on each piece of NF using $NaBH_4$, which served as both the reducing agent and a source of boron. The resultant solution was aged for 30 min. The precipitate was collected by filtration. The Fe_2B NWs/NF and collected Fe_2B powder were rinsed with deionized water and ethanol, dried in vacuo at 30 ^oC, and stored in a glove box (Mbraun, Munich, Germany) circulated with Ar. The Fe_2B nanoparticles (NPs)/NF was synthesised using the same method as for the Fe_2B NWs/NF except the former was performed in the absence of a magnetic field. The mass loadings of Fe_2B NWs and NPs were both ~ 1 mg. Since the

geometric area of the NF substrate (both sides) is about 4 cm^2, the amouts of Fe_2B NWs and NPs loading were 0.25 mg/cm^2.

For comparison purposes, Fe NPs/NF was prepared by an electrodeposition process. The electrodeposition of Fe was conducted in 6 mM $Fe(NO_3)_3$ under a constant potential of –1.0 V with NF, Ag/AgCl and Pt plate serving as the working, reference, and auxiliary electrodes. After electrodeposition for 600 s, each Fe NPs/NF was carefully removed from the electrolyte and treated using a procedure similar to that for the Fe_2B NWs/NF catalyst. The loading amout of Fe NPs was about 0.25 mg/cm^2.

Characterization

Elemental analysis was performed using inductively coupled plasma-optical emission spectroscopy (ICP-OES, Optima 5300DV, Perkin Elmer). The phase structures of the catalyst samples were analyzed with Cu Kα radiation (λ = 1.54178 Å) from an X-ray diffractometer (XRD, D8 advance diffractometer). The morphology and microstructure of the catalyst were examined with a field-emission scanning electron microscopy (SEM, JEOL JSM 6700F) and a transmission electron microscopy (TEM, JEOL JEM 2100F), both equipped with the energy dispersive X-ray spectroscopic (EDS) mode (Oxford, INCA). Fourier transform infrared (FT-IR) spectra were recorded on a Thermo-Nicolet 6700 spectrometer. The chemical states of the constituent elements of the catalyst were analyzed with an XPS instrument equipped with a monochromatized Al source (1486.6 eV) and a 160 mm concentric hemispherical energy analyzer (Shimadzu, AXIS Ultra Supra). The binding energies (BEs) were determined using the C 1s peak (at 284.8 eV) from adventitious carbon as the reference. Hydrophilicity was measured using a contact angle measurement system (KSV instruments).

Electrochemical measurements

All electrochemical measurements were performed in a conventional three-electrode cell using a CHI 760E electrochemical analyzer. The OER catalysts, a graphite plate and a Hg/HgO were used as the working, counter, and reference electrode. The potentials measured *vs.* Hg/HgO were converted to reversible hydrogen electrode (RHE), according to the equation, $E_{RHE} = E_{Hg/HgO} + 0.098 + 0.059 \times pH$. The electrochemical performance of the catalysts was investigated in an oxygen-saturated 1 M KOH solution. Before recording the polarization curves, potential was cycled five times between 1.22 and 1.72 V *vs.* RHE at 100 mV/s. The polarization curves were recorded by scanning from 1.22 to 1.72 V *vs.* RHE at 2 mV/s with 90% *iR* compensation. The electrochemical impedance spectroscopy was performed at open circuit potential with an amplitude of 5 mV in the frequency range from 100 kHz to 0.1 Hz. The curve fitting was performed by Zview2 software. The electrochemical surface areas (ECSA) of the catalysts were calculated from their double-layer capacitance (C_{dl}), which were determined from the scan-rate dependence of capacitive current.[1] The roughness factor (RF) was calculated by dividing the estimated ECSA by the geometric area of the electrode in the electrolyte (1 cm^2). The mass activity of the Fe_2B NWs/NF catalyst was calculated according to mass activity = $J_{ECSA} \times A/m$, where J_{ECSA} is the current density normalized to the estimated ECSA of the Fe_2B NWs/NF catalyst, A the estimated ECSA of the Fe_2B NWs/NF catalyst, and m the loading mass of Fe_2B NWs.

$$A = \frac{The\ total\ specific\ capacitance\ of\ Fe_2B\ NWs/NF}{The\ specific\ capacitance\ of\ per\ ECSA} = \frac{1.2\ mF/cm^2}{40\ uF/cm^2 per\ cm^2} = 30\ cm^2$$

The turnover frequency (TOF) was defined as the number of O_2 molecules produced per second per active site:

$$n_{O_2} = (J_{ECSA}\frac{mA}{cm^2})(\frac{1\ C/s}{1000\ mA})(\frac{1\ mol\ e^-}{96485.3\ C})(\frac{1\ mol\ O_2}{4\ mol\ e^-})(\frac{6.022 \times 10^{23}\ O_2\ molecules}{1\ mol\ O_2})$$

$$= (1.56 \times 10^{15}\frac{1}{s} per \frac{mA}{cm^2}) \times (J_{ECSA}\frac{mA}{cm^2})$$

We assume all of the surface Fe and B atoms as the number of active sites. The volume of each unit cell of Fe_2B (eight iron and four boron atoms) is 111.66 Å^3.[2] Thus,

$$n_{active\ sites} = \left(\frac{12\ atoms/unit\ cell}{111.66\ Å^3/unit\ cell}\right)^{2/3} = 2.26 \times 10^{15}\ atoms/cm^2$$

$$TOF = \frac{(1.56 \times 10^{15}\frac{1}{s}per\frac{mA}{cm^2}) \times (J_{ECSA}\frac{mA}{cm^2})}{(2.26 \times 10^{15}\ atoms/cm^2) \times (A\ cm^2)} = 0.023 \times J_{ECSA}\ (s^{-1})$$

Determination of Faradaic efficiency

The amount of O_2 generated in OER was measured using a classic water drainage method.[3] The Faradaic efficiency was deduced by comparing the experimentally measured gas amount with the theoretically calculated value. Specifically, the efficiency was calculated from ($m \times n \times F$)/($I \times t$), where m is the product in moles, n the number of electrons transferred, F the Faraday constant, I the current value, and t the reaction time.

Computational methods

All calculations in this work were performed with the Vienna ab initio simulation package (VASP) based on the density functional theory (DFT).[4] The generalized gradient approximation was used for the exchange-correlation energy. The spin polarization was taken into account with a cutoff energy of 400 eV. A vacuum region of 18 Å was used to eliminate interactions between the neighboring slab models. Monkhorst k-point meshes of 3 × 3 × 1 were used for the Brillouin-zone integrations of slab supercell models. The total energy converges within an error of 1×10^{-5} eV/atom, and all atoms were relaxed until the residual force was less than 0.02 eV/Å during relaxation. The DFT-D2 method proposed by Grimme et al. was adopted to describe the van der Waals interactions.[5] The OER performance was evaluated by computing the change of Gibbs free energy (ΔG) based on the spin-polarized calculation via the following equation:

$$\Delta G = \Delta E + \Delta E_{ZPE} + \Delta H - T\Delta S$$

where ΔE is the energy difference for a given intermediate before and after adsorbed on the surface of slab models, ΔE_{ZPE}, ΔH and ΔS the differences in the zero-point energy, enthalpy and entropy between the adsorbed state and the corresponding free-standing state.

Results and Discussion

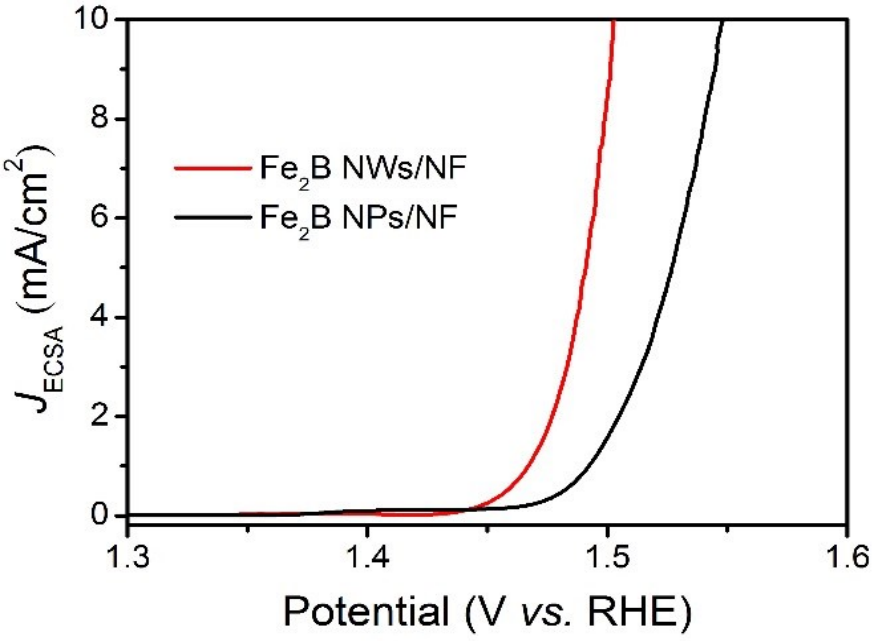

Fig. S1 OER polarization curves of the Fe_2B NWs/NF and Fe_2B NPs/NF.

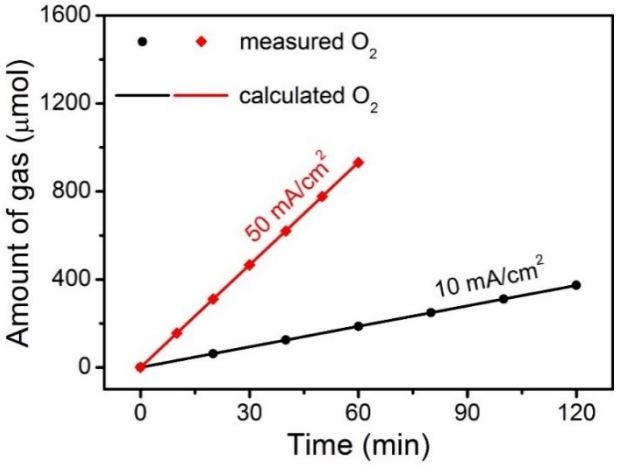

Fig. S2 Experimentally measured O_2 evolution *vs.* theoretically calculated quantities under constant current densities of 10 and 50 mA/cm^2.

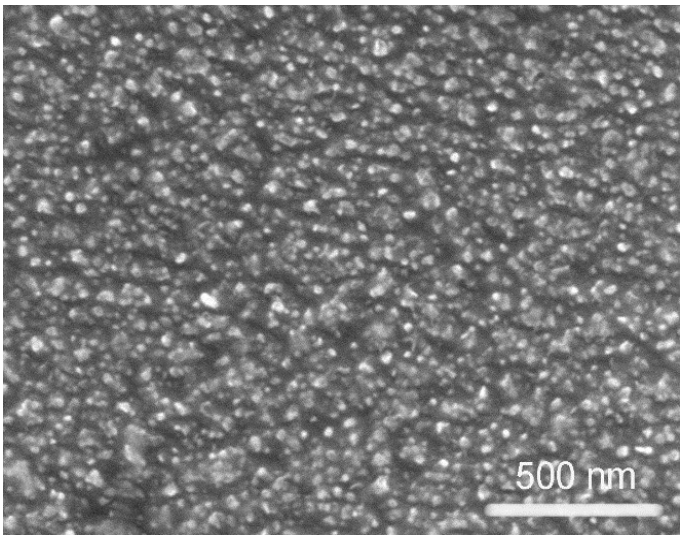

Fig. S3 A field-emission SEM image of the Fe_2B NPs/NF.

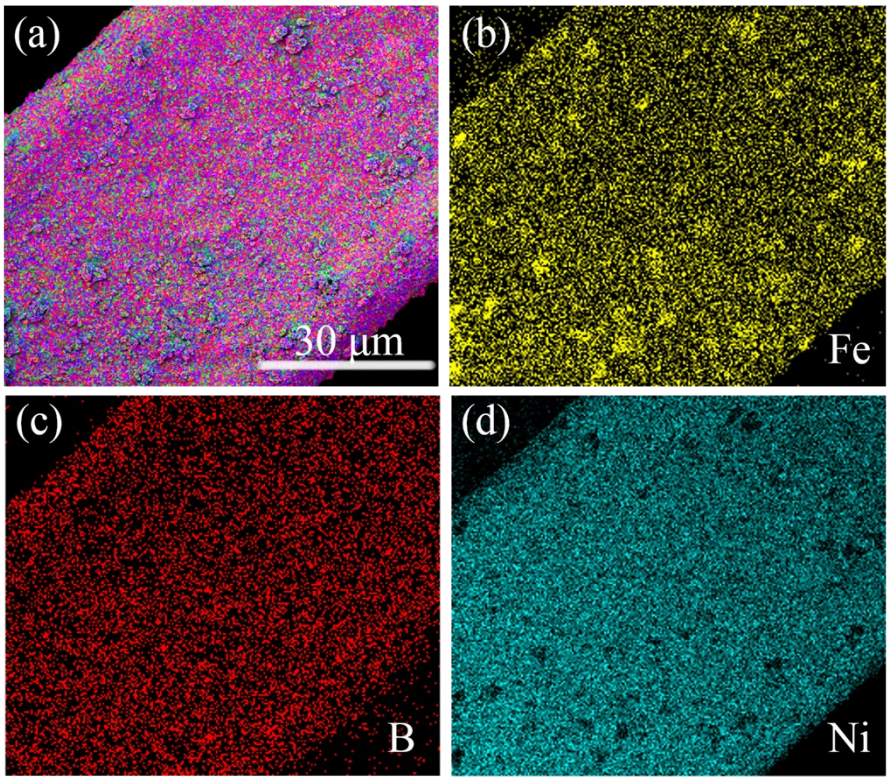

Fig. S4 A field emission-SEM image (a) of the Fe_2B NWs/NF and the EDS elemental maps corresponding to Fe (b), B (c), and Ni (d).

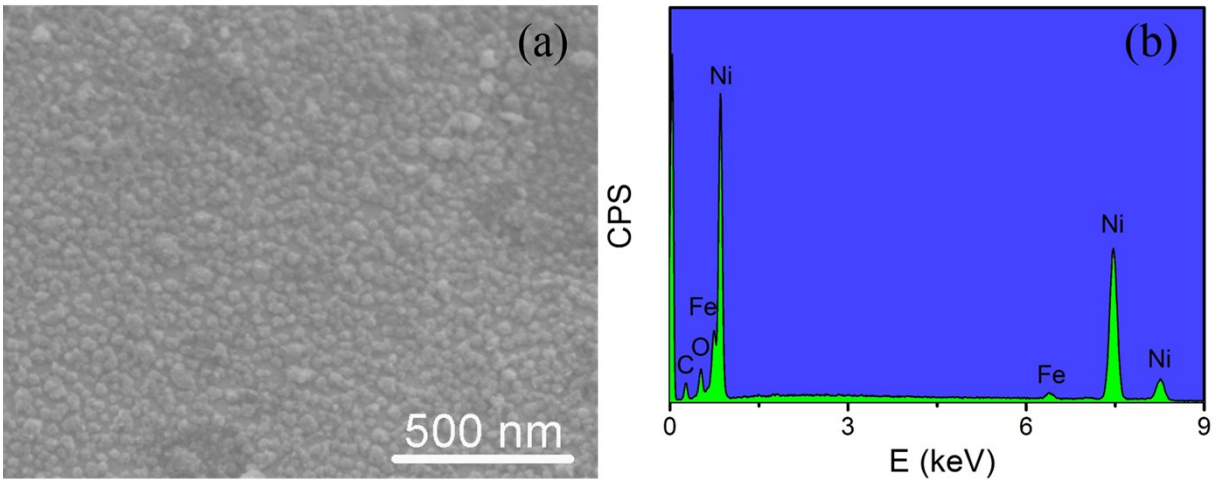

Fig. S5 (a) A field-emission SEM image and (b) its corresponding EDS spectrum of the Fe NPs/NF.

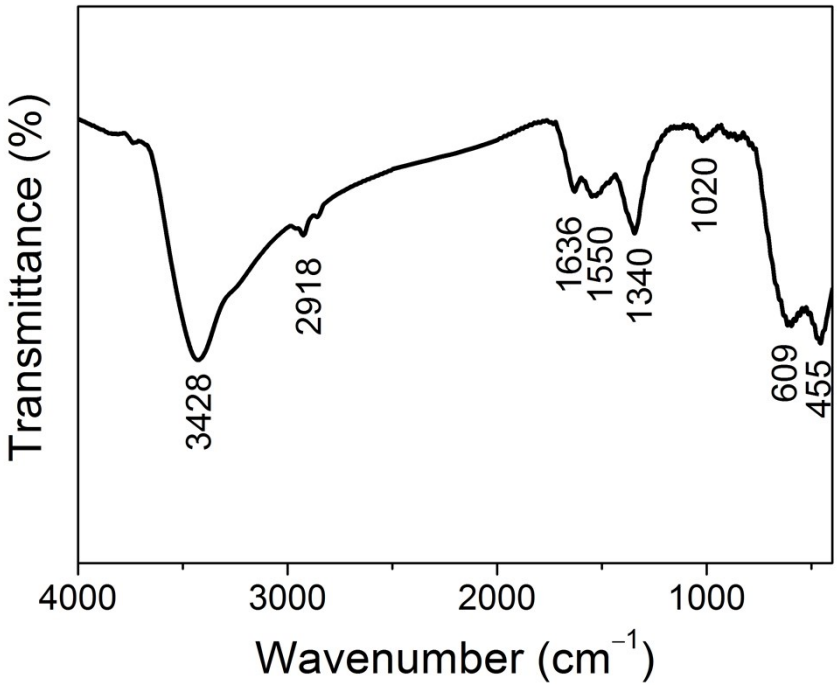

Fig. S6 An FT-IR spectrum of the Fe_2B NWs/NF after OER.

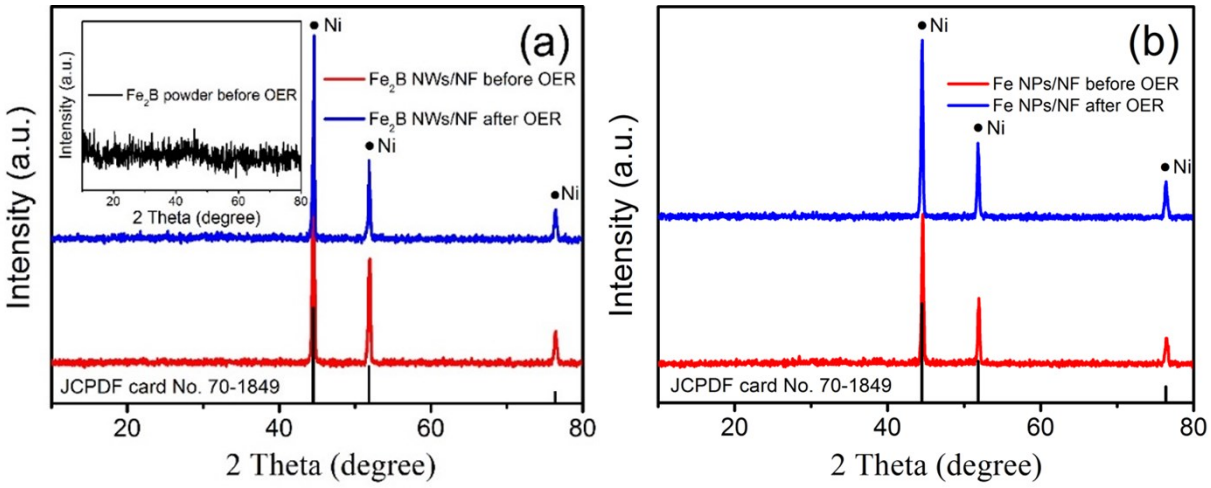

Fig. S7 XRD patterns of (a) Fe_2B NWs/NF and (b) Fe NPs/NF before and after OER. The insert in (a) shows the XRD pattern of the corresponding Fe_2B powder scraped from the NFs before OER.

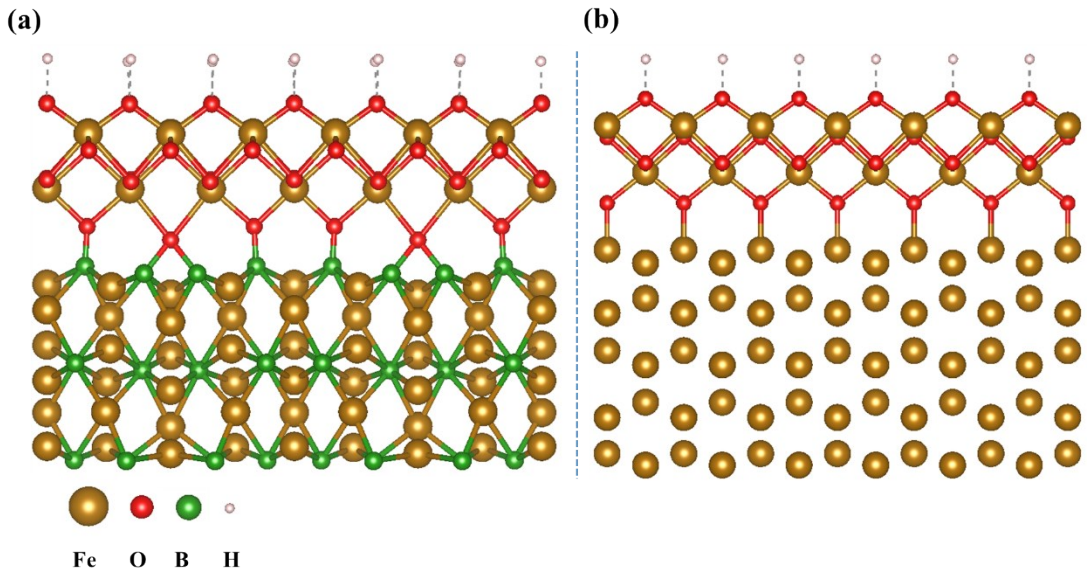

Fig. S8 Crystal structures of slab models of FeOOH@Fe_2B (a) and FeOOH@Fe (b).

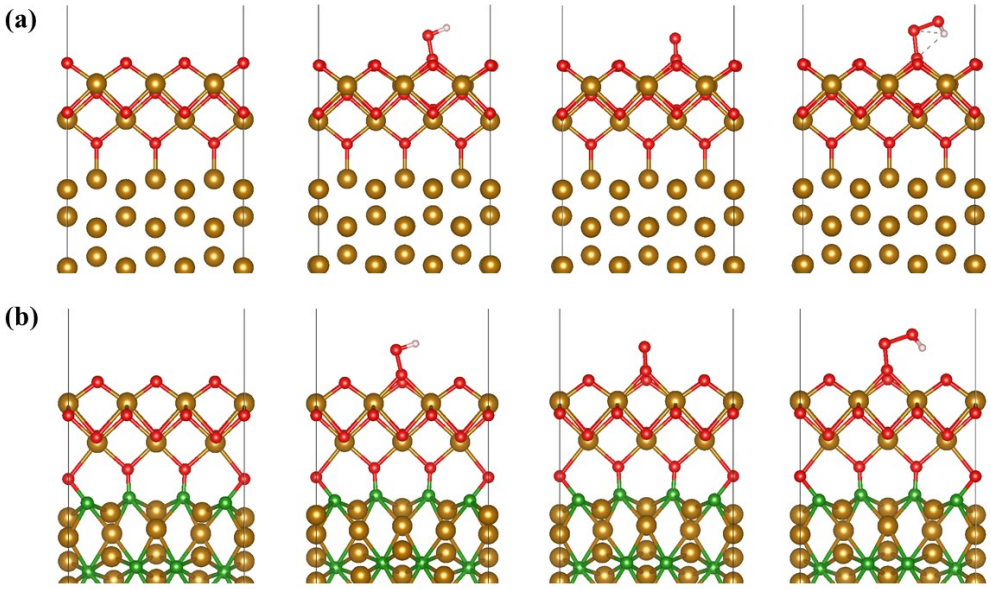

Fig. S9 Crystal structures of OER intermediates of FeOOH@Fe (a) and FeOOH@Fe_2B (b).

Table S1. Summary of charge transfer resistance (R_{ct}), double-layer capacitance (C_{dl}), electrochemical surface area (ECSA), and roughness factor (RF) for various catalysts in this study.

	Fe_2B NWs/NF	Fe NPs/NF	NF
R_{ct} (Ω)	4.76	26.89	8.88
C_{dl} (mF/cm^2)	1.20	0.85	0.59
ECSA (cm^2)	30	21.25	14.75
RF	30	21.25	14.75

Table S2. Summary of thermal correcting energies for OER.

Species	$\Delta E_{ZPE} + \Delta H - T\Delta S$ (eV) (298K)	
	FeOOH@Fe	FeOOH@Fe_2B
O*	0.08	0.06
OH*	0.33	0.37
OOH*	0.43	0.41
H_2 (g)		–0.14
H_2O (g)		–0.02

Table S3. Total energies of pure surfaces in the FeOOH@Fe and FeOOH@Fe_2B models for OER

	E* (eV)	E_{OH*} (eV)	E_{O*} (eV)	E_{OOH*} (eV)
FeOOH@Fe	–736.993	–747.736	–741.131	–750.155
FeOOH@Fe_2B	–699.940	–710.294	–704.551	–713.463

Reference

1. a) A. J. Bard, L. R. Faulkner in *Electrochemical Methods: Fundamentals and Applications*, 2nd ed; Wiley, New York, 2001. b) C. C. L. McCrory, S. Jung, J. C. Peters, T. F. Jaramillo, *J. Am. Chem. Soc.*, 2013, **135**, 16977–16987. c) F. Song, X. Hu, *Nat. Commun*., 2014, **5**, 4477.
2. H. Li, P. Wen, Q. Li, C. Dun, J. Xing, C. Lu, S. Adhikari, L. Jiang, D. L. Carroll, S. M. Geyer, *Adv. Energy Mater.*, 2017, **7**, 1700513.
3. N. Xu, G. Cao, Z. Chen, Q. Kang, H. Dai, P. Wang, *J. Mater. Chem. A*, 2017, **5**, 12379–12384.
4. G. Kresse, J. Furthmuller, *Phys. Rev. B: Condens. Matter Mater. Phys.*, 1996, **54**, 11169.
5. S. Grimme, *J. Comput. Chem*., 2006, **27**, 1787–1799.